

## ORIGINAL ARTICLE

# HER2 exon 20 insertions in non-small-cell lung cancer are sensitive to the irreversible pan-HER receptor tyrosine kinase inhibitor pyrotinib

Y. Wang<sup>1†</sup>, T. Jiang<sup>1†</sup>, Z. Qin<sup>2†</sup>, J. Jiang<sup>3</sup>, Q. Wang<sup>3</sup>, S. Yang<sup>1</sup>, C. Rivard<sup>4</sup>, G. Gao<sup>1</sup>, T. L. Ng<sup>4</sup>, M. M. Tu<sup>5,6</sup>, H. Yu<sup>4</sup>, H. Ji<sup>1,2‡</sup>, C. Zhou<sup>1‡</sup>, S. Ren<sup>1,4\*‡</sup>, J. Zhang<sup>7</sup>, P. Bunn<sup>4</sup>, R. C. Doebele<sup>4</sup>, D. R. Camidge<sup>4</sup> & F. R. Hirsch<sup>4</sup>

<sup>1</sup>Department of Medical Oncology, Shanghai Pulmonary Hospital, Tongji University School of Medicine, Shanghai; <sup>2</sup>Institute of Biochemistry and Cell Biology, Shanghai Institutes for Biological Sciences, Chinese Academy of Sciences, Shanghai; <sup>3</sup>Department of Medical Affairs, Hengrui Pharmaceutical Company, Shanghai, China; <sup>4</sup>Departments of Medicine, Medical Oncology, University of Colorado Anschutz Medical Campus, Aurora; <sup>5</sup>Department of Surgery (Urology), University of Colorado Anschutz Medical Campus, Aurora; <sup>6</sup>University of Colorado Comprehensive Cancer Center, Aurora; <sup>7</sup>Division of Hematology, Oncology and Blood & Marrow Transplantation, Department of Internal Medicine, Holden Comprehensive Cancer Center, University of Iowa Carver College of Medicine, Iowa City, USA

\*Correspondence to: Prof. Shengxiang Ren, Department of Medical Oncology, Shanghai Pulmonary Hospital, Tongji University School of Medicine, No. 507, Zheng Min Road, Shanghai 200433, China. Tel: +86-21-65115006; E-mail: harry\_ren@126.com

†The first three authors contributed equally to this work.

‡These authors contributed equally as senior authors.

**Background:** Effective targeted therapy for non-small-cell lung cancer (NSCLC) patients with human epidermal growth factor receptor 2 (*HER2*) mutations remains an unmet need. This study investigated the antitumor effect of an irreversible pan-HER receptor tyrosine kinase inhibitor, pyrotinib.

**Patients and methods:** Using patient-derived organoids and xenografts established from an *HER2*-A775\_G776YVMA-inserted advanced lung adenocarcinoma patient sample, we investigated the antitumor activity of pyrotinib. Preliminary safety and efficacy of pyrotinib in 15 *HER2*-mutant NSCLC patients in a phase II clinical trial are also presented.

**Results:** Pyrotinib showed significant growth inhibition of organoids relative to afatinib *in vitro* ( $P = 0.0038$ ). In the PDX model, pyrotinib showed a superior antitumor effect than afatinib ( $P = 0.0471$ ) and T-DM1 ( $P = 0.0138$ ). Mice treated with pyrotinib displayed significant tumor burden reduction (mean tumor volume,  $-52.2\%$ ). In contrast, afatinib ( $25.4\%$ ) and T-DM1 ( $10.9\%$ ) showed no obvious reduction. Moreover, pyrotinib showed a robust ability to inhibit pHER2, pERK and pAkt. In the phase II cohort of 15 patients with *HER2*-mutant NSCLC, pyrotinib 400 mg resulted in a objective response rate of  $53.3\%$  and a median progression-free survival of 6.4 months.

**Conclusion:** Pyrotinib showed activity against NSCLC with *HER2* exon 20 mutations in both patient-derived organoids and a PDX model. In the clinical trial, pyrotinib showed promising efficacy.

**Clinical trial registration:** NCT02535507.

**Key words:** non-small-cell lung cancer, *HER2* mutations, pyrotinib, patient-derived organoids, clinical trial

## Introduction

Mutations in the human epidermal growth factor receptor 2 (*HER2*, *ERBB2*) have been identified as oncogenic drivers and occur in 2%–3% of non-small-cell lung cancer (NSCLC) [1–6], and as high as 6.7% in EGFR/ALK/ROS1 triple-negative NSCLC [7]. *HER2* mutations most commonly consist of a 12 bases

pair in-frame insertion YVMA (p.A775\_G776insYVMA) in exon 20, leading to downstream activation of the PI3K-AKT and RAS-MAPK pathways [1, 4]. Historically, patients with *HER2*-mutant NSCLC have a median overall survival (OS) of 1.6–1.9 years from the time of stage IV diagnosis [5, 6]. Several patient reports and series reporting on *HER2*-targeted agents in patients with

HER2-mutant NSCLC, including afatinib, dacomitinib, neratinib and trastuzumab, have shown limited clinical activity [6, 8–12]. Thus, chemotherapy remains the main strategy for this patient population [13]. However, our previous study demonstrated that HER2-mutant lung cancers treated with first-line pemetrexed-based chemotherapy had an inferior outcome compared with lung cancers with an *ALK* or *ROS1* rearrangement [14]. Therefore, there is an urgent need for effective HER2-targeted drugs to improve the long-term outcome in this subset of patients.

Pyrotinib is an oral, irreversible pan-HER receptor tyrosine kinase inhibitor (TKI) with activity against epidermal growth factor receptor (EGFR)/HER1 and HER2. Preclinical data together with phase I clinical data suggest that pyrotinib can irreversibly inhibit multiple HER receptors and effectively inhibit the proliferation of HER2-overexpressing cells *in vitro* and *in vivo* [15, 16]. In this study, we utilized a patient-derived organoid and a patient-derived xenografts (PDX) model to test the antitumor effect of pyrotinib in the preclinical setting. We then validated those preclinical findings in patients enrolled in a phase II clinical trial.

## Methods

### Patient-derived tumor organoid culture

The primary organoids were established using previously described culture methods [17]. Briefly, eligible biopsy pieces were minced with scissors and digested in 5 ml of 5 mg/ml collagenase type II (Invitrogen) in Advanced DMEM/F12 (ADMEM/F12) and digested for 2–3 h at 37°C with gentle shaking. Dissociated cells were washed and then seeded in growth factor-reduced Matrigel (BD biosciences). Organoids were passaged at a 1 : 3 dilution every week either via trituration with a glass Pasteur pipet or dissociation with TrypLE (Sigma-Aldrich) for 5 min at 37°C.

### Patient-derived xenografts studies

Mice were treated in accordance with Good Animal Practices and carried out with the approval of the Animal Ethics Committee at Tongji University School of Medicine. For the xenografts, tumor fragments 15–30 mm<sup>3</sup> in size were subcutaneously implanted into the right flanks of BALB/c Nude mice. When the tumors reached 150–250 mm<sup>3</sup>, tumor-bearing mice were randomly divided into 6 groups (12 in the control group and 6 in each treatment group, including the 5 mg/kg pyrotinib, 20 mg/kg pyrotinib, 80 mg/kg pyrotinib, 15 mg/kg afatinib and 10 mg/kg T-DM1 groups, respectively; [supplementary Table S1](#), available at *Annals of Oncology* online). Tumor volumes and body weight were measured every 3–4 days. Treatment was discontinued when tumor volume exceeded 2000 mm<sup>3</sup>, body weight loss was >20%, or the mouse were moribund and had poor oral intake. Mice euthanized for events unrelated to tumor burden were excluded from the final analysis. Comparison of treatment arms for the *in vivo* mouse xenograft studies was carried out using one-way ANOVA in GraphPad Software.

### In vivo pharmacokinetic study

Samples of BALB/c nude mice utilized for pharmacokinetic study were collected after a single dose of pyrotinib ([supplementary Table S1](#), available at *Annals of Oncology* online). Drug concentrations in the blood and tumor tissue were analyzed by liquid chromatograph-mass spectrometer/mass spectrometer (LC–MS/MS), as described previously [15].

## Cell viability, proliferation assay, IHC, IF and western blot

See the [supplementary materials](#), available at *Annals of Oncology* online for details.

## Clinical trial

We initiated a phase II clinical study to evaluate the safety and efficacy of pyrotinib in patients with advanced HER2-mutant NSCLC without standard therapy options (ClinicalTrials.gov: NCT02535507). Eligible patients included adults (aged ≥18 and ≤80 years) with histologically confirmed advanced HER2-mutant NSCLC and progression through at least one standard regimen of therapy. Patients were required to have an Eastern Cooperative Oncology Group performance status of 0–2 and at least one measurable lesion by Response Evaluation Criteria in Solid Tumors (RECIST 1.1). Prior HER2-targeted therapy was allowed. Only adequately locally treated and asymptomatic brain metastases were allowed. HER2 mutation was tested using ADx HER2 Mutation Detection Kit (Amoy Diagnostics, Xiamen, China) or NGS, and confirmed by DNA direct sequencing if needed. Eligible HER2 variations included HER2 mutations in exon 20 and exon 19 (tyrosine kinase domain). This study was approved by the Ethics Committee of Shanghai Pulmonary Hospital, and a written informed consent was obtained from each participant before initiation of any study-related procedure. The study is sponsored by Hengrui Pharmaceuticals (Shanghai, China), and conducted in accordance with the Declaration of Helsinki and Good Clinical Practices.

Estimated enrollment of 13 of the first stage was determined by optimal two-stage design and finally 15 eligible patients were enrolled. All the patients were Chinese diagnosed in Shanghai Pulmonary Hospital. Enrolled patients received recommended doses of pyrotinib (400 mg, p.o.) daily according to the recommended phase II dose (RP2D) from phase I clinical trial [16], until intolerable toxicity, disease progression, death or withdrawal of consent. Treatment continuation beyond disease progression was allowed based on the fact that a number of patients with radiologic gradual progression via RECIST can still benefit from therapy continuation. Tumor response was evaluated 4 weeks after the initiation of pyrotinib treatment and then every 6–8 weeks afterwards according to RECIST 1.1. Complete response (CR) or partial response (PR) had to be confirmed at least 4 weeks after initial response. The duration of responses was measured from the time of the first documentation of response to the date of disease progression.

The primary end point of this study was objective response rate (ORR). Secondary end points included progression-free survival (PFS), OS, safety and tolerability of pyrotinib. PFS was defined as the time interval from the date of treatment initiation to documented disease progression or death of any cause. OS was defined as the time from treatment initiation of pyrotinib to death of any cause. All adverse events were assessed and classified by grade according to the national cancer institute common terminology criteria for adverse events (version 4.0).

## Results

### Activity of pyrotinib in HER2-mutant patient-derived organoids

We successfully established patient-derived lung cancer organoids (Figure 1A and [supplementary Figure S1](#), available at *Annals of Oncology* online) from a 42 years old female with HER2-A775\_G776YVMA-inserted advanced lung adenocarcinoma. H&E, IHC and immunofluorescence staining results of the organoid confirmed its epithelial origin (Figure 1A and B), and direct sequencing of a representative organoid confirmed HER2

A775\_G776YVMA insertion (Figure 1C), suggesting that genomic characterization of the organoids was identical to the parental tumor from which they were derived.

To demonstrate the activity of pyrotinib in lung cancer cells with HER2 A775\_G776YVMA insertion, we carried out cell viability and proliferation assays using the established organoids. The organoids converted to 2D cells were challenged with drug for 72 h, and drug responses were determined by quantifying cell viability measured by CellTiter-Glo (Promega) Luminescent Cell Viability Assay. Drug response curves of the organoids treated with two dual EGFR/HER2 inhibitors, afatinib and pyrotinib showed that the  $IC_{50}$  of pyrotinib was similar to that of afatinib (112.5 and 89.1 nM;  $P > 0.05$ ) (Figure 1D). However, when the organoids were treated with afatinib and pyrotinib at plasma concentrations of 29 nM [ $(C_{afatinib}: 21.1 \text{ ng/ml}) / (MW_{afatinib}: 718.08 \text{ g/mol}) \times 1000$ ] and 180 nM [ $(C_{pyrotinib}: 147 \text{ ng/ml}) / (MW_{pyrotinib}: 815.22 \text{ g/mol}) \times 1000$ ], respectively, adopted from the *in vivo* plasma concentrations of the two drugs in previous phase I clinical studies [16, 18], pyrotinib showed significantly higher inhibition of cell growth than afatinib ( $P = 0.0038$ ; Figure 1E). The 3D organoids treated with vehicle (DMSO), afatinib (29 nM) and pyrotinib (180 nM) showed similar results. Compared with afatinib, pyrotinib at the recommended plasma concentration of human level inhibited the cell growth more significantly (Figure 1F).

### **In vivo activity of pyrotinib in a PDX model**

We next determined whether pyrotinib could significantly inhibit tumor growth *in vivo*. Five groups of mice were treated with HER2 inhibitors, and one group received vehicle for 24 days. Three groups of mice were treated with pyrotinib orally daily at 5, 20 and 80 mg/kg, respectively. Dose-dependent tumor inhibition was observed (Figure 2A and [supplementary Figure S2A](#), available at *Annals of Oncology* online). Residual tumor volume of the mice treated with pyrotinib at 80 mg/kg was minimal (Figure 2A). Waterfall plots show that pyrotinib treatment (80 mg/kg) significantly shrank tumors by 24 days in the HER2 exon 20 insertion PDX models (Figure 2B), and no significant decrease in body weight was seen (Figure 2C), indicating pyrotinib was safe and effective in inhibiting tumor growth *in vivo*.

The remaining two mouse cohorts were treated with afatinib at 15 mg/kg orally daily and T-DM1 at 10 mg/kg intravenously on day 0, 7, 14 and 21. We found that when pyrotinib was administered at a dose of 80 mg/kg, it resulted in more profound tumor regression than afatinib ( $P = 0.0471$ ) and T-DM1 ( $P = 0.0138$ ) (Figure 2D and [supplementary Figure S2B](#), available at *Annals of Oncology* online). As shown in Figure 2E, pyrotinib-treated mice displayed significant reduction of tumor burden (mean % tumor volume change,  $-52.2\%$ ). In contrast, mice receiving afatinib (mean % tumor volume change,  $+25.4\%$ ) or T-DM1 (mean of % tumor volume change,  $+10.9\%$ ) showed no significant reduction of tumor burden, although they both inhibited tumor growth compared with the vehicle control (Figure 2E). Meanwhile, the weight of mice receiving afatinib at 15 mg/kg significantly decreased compared with mice receiving either vehicle control or pyrotinib of 80 mg/kg ( $P < 0.0001$ ) (Figure 2F).

As shown in Figure 2G and H, the average plasma drug concentration of the mice treated with pyrotinib was 2316.7 ng/ml,

which was significantly higher than that of mice treated with afatinib (76.9 ng/ml;  $P < 0.0001$ ). The pyrotinib concentration in the tumor of the 80 mg/kg group was not available due to a low volume of tumor tissue after 24 days of pyrotinib treatment. In IHC, pyrotinib inhibited phosphorylation of HER2 and its downstream proteins. The tumors that had been treated with pyrotinib for 24 days showed definite reduction of pHER2, pERK and pAkt when compared with the vehicle (Figure 2I). Afatinib and T-DM1 also showed the ability to block the same HER2 downstream signaling pathways ([supplementary Figures S2C and S3](#), available at *Annals of Oncology* online). IHC staining of VEGFR2 was also carried out on tumors in pyrotinib treatment group but no significant reduction of VEGFR2 phosphorylation was observed ([supplementary Figure S4](#), available at *Annals of Oncology* online).

### **PK/PD correlation of pyrotinib in PDX model**

To assess pharmacokinetics/pharmacodynamics (PK/PD) correlation of pyrotinib, we carried out drug concentration measurement and IHC on tumors harvested from mice exposed to pyrotinib (80 mg/kg) for 2, 6 and 24 h. Pharmacokinetic parameters of pyrotinib in mice were shown in [supplementary Table S3](#), available at *Annals of Oncology* online. Pyrotinib plasma concentration peaked at 2 h after dosing (3433 ng/ml). Furthermore, concentration of pyrotinib in tumors reached maximum at 6 h after dosing, and at the same time, pHER2 was maximally inhibited (Figure 3A and B). IHC and western blot were used to detect expression of HER2 and its downstream proteins, including ERK and Akt. The results showed that phosphorylation of these proteins was significantly inhibited at 6 h after dosing (Figure 3C–F).

### **HER2-mutant lung cancer patients response to pyrotinib**

Efficacy of pyrotinib in patients with advanced HER2-mutant lung cancer was evaluated in a phase II clinical study. HER2 mutations were detected by ARMS or NGS. The 15 patients enrolled from July 2015 to September 2016 received pyrotinib treatment (400 mg). Among them, one patient received a dose of 320 mg due to his age of 78 years and renal insufficiency. The clinical characteristics and previous anticancer therapies are summarized in [supplementary Tables S4, S5 and Figure S5](#), available at *Annals of Oncology* online. Ten of them had HER2 A775\_G776insYVMA insertion. None of the subjects received pyrotinib as their first-line therapy, and the median number of previous treatment lines was 2.

Among 15 patients amenable for response evaluation, eight (53.3%) of them had a partial response and three (20.0%) had stable disease (Figure 4A). The median time to response was 1.0 months and median duration of response was 7.2 months (range 2.1–20.0 months). The median PFS time was 6.4 months (95% CI 1.60–11.20). The ORR and PFS of the 10 patients with HER2 A775\_G776insYVMA (Figure 4B and C) were 50% and 4.1 months (95% CI 1.42–6.10), respectively. The range of PFS was 1.7–23.4 months with 3 patients remaining on therapy for  $>1$  year. Patients with HER2 G776C, G776>VC, or L755P, also responded to pyrotinib. PFS of one patient with P780\_Y781insGSP exceeded 1 year. But the patient with



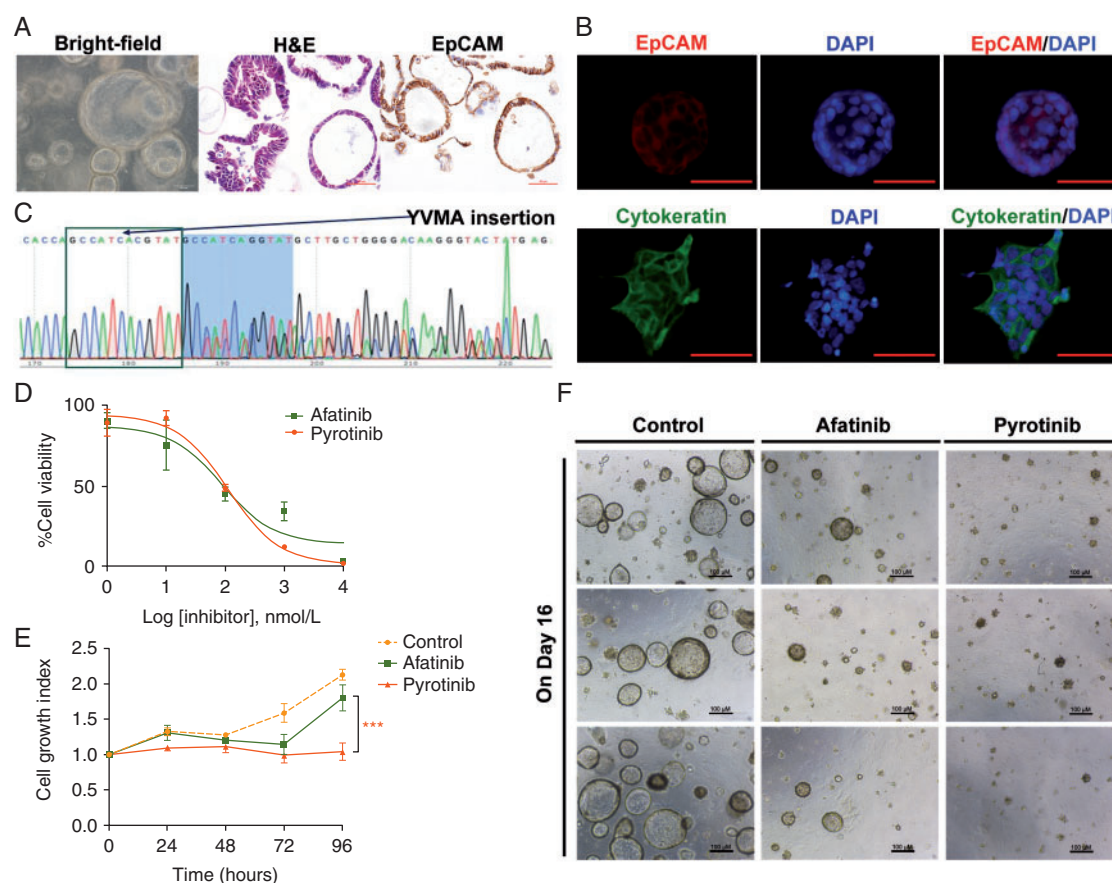


**Figure 1.** Activity of pyrotinib in HER2-mutant patient-derived organoids. (A, B) 3D organoids in bright field ( $10 \times 10$ ), and H&E and IHC results of representative organoids suggested epithelial origin. (C) Sequencing results of representative organoids showed *HER2* A775\_G776insYVMA, indicating that the genomic characterization of this patient-derived *in vitro* models was identical to the parental tumor. (D) Drug response curves of the organoids treated with the dual EGFR/HER2 inhibitors (afatinib and pyrotinib, respectively) showed that the  $IC_{50}$  of afatinib and pyrotinib were 89.1 and 112.5 nM. Cell viability was measured by a CellTiter-Glo (Promega) Luminescent Cell Viability Assay after 72 h of treatment. (E) Cell growth curves of the organoids treated with vehicle (DMSO), afatinib (29 nM<sup>#</sup>) and pyrotinib (180 nM<sup>#</sup>) showed that compared with afatinib, pyrotinib at plasma concentration inhibited the cell growth more significantly ( $*P = 0.0038$ ). <sup>#</sup>The concentrations were adopted from the *in vivo* plasma concentrations of the 2 drugs in previous phase I clinical studies, e.g. ( $C_{afatinib}$ : 21.1 ng/ml)/(MW<sub>afatinib</sub>: 718.08 g/mol)  $\times 1000 = 29$  nM; ( $C_{pyrotinib}$ : 147 ng/ml)/(MW<sub>pyrotinib</sub>: 815.22 g/mol)  $\times 1000 = 180$  nM. (F) Representative images (three repeated well) of the 3D organoids treated with vehicle (DMSO), afatinib (29 nM) and pyrotinib (180 nM) on day 16 after dosing.

G776>IC failed to response to pyrotinib (Figure 4B). Two patients (2/15, 13%) had brain metastases before enrollment. One of them discontinued pyrotinib 4 weeks later due to the progression of the lung lesion and the other achieved stable disease after pyrotinib treatment. Of 13 patients without brain metastasis at baseline, three (3/13, 23%) had intracranial progression. Only one patient had received HER2-targeted therapy (afatinib 40 mg daily) before enrollment and he responded to pyrotinib after disease progression on afatinib.

At the last follow-up date of December 2017, four patients were still on pyrotinib treatment (Figure 4D). PFS of two of them did not reach (more than 23.4 months and more than 8.5 months) and two others continued to take pyrotinib after gradual progression or isolated brain metastasis assessed by their doctors (postprogressive treatment was not calculated in PFS). Five patients (33%) remained on pyrotinib for more than 1 year and two patients (13%) for more than 18 months. Six patients (40%) were still alive at the last follow-up, and the median overall survival (OS) was 12.9 months (95% CI 2.05–23.75) (Figure 4D).

Pyrotinib related adverse events of any grade were observed in nine patients (60%). No one had received prophylactic antidiarrheal treatment but four patients (27%) did suffer grade 1–2 diarrhea. Other adverse events included decreased hemoglobin (27%), hypocalcemia (27%), fatigue (14%), rash (14%), increased AST (14%), paronychia (7%), nausea (7%), increased ALT (7%), dyspnea (7%), vomiting (7%), hyperbilirubinemia (7%) and leukopenia (7%). They all were grade 1–2 and no dose reduction or dose discontinuation occurred due to adverse events (supplementary Table S6, available at *Annals of Oncology* online).

Figure 4E and F are two representative cases showing response to pyrotinib. The first patient was a 78-year-old Chinese male diagnosed with stage IV lung adenocarcinoma with bilateral intrapulmonary metastases in Shanghai Pulmonary Hospital in 2015. He received two cycles of chemotherapy, then developed disease progression. He was found to have an *HER2* exon 20 A775\_G776insYVMA mutation, then enrolled into this clinical trial and received a lower dose of pyrotinib 320 mg oral daily due to his age and renal

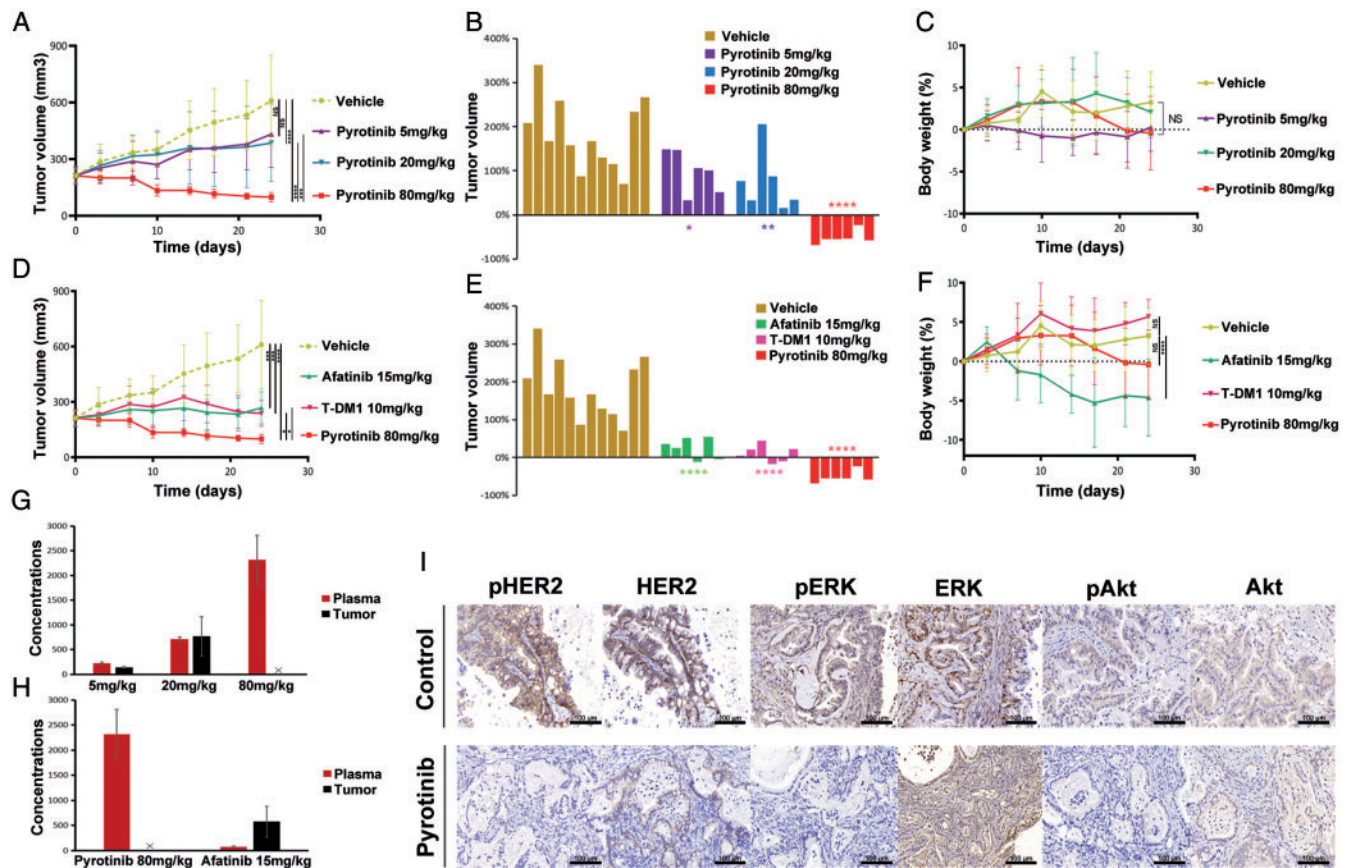


**Figure 2.** *In vivo* activity of pyrotinib in PDX models. (A) Tumor volume curves of the PDX models treated with vehicle, and different doses of pyrotinib. (B) Tumor volume changes among mice treated with vehicle, and different doses of pyrotinib by 24 days. (C) Body weight changes among mice treated with vehicle, and different doses of pyrotinib. (D) Tumor volume curves of the PDX models treated with vehicle, pyrotinib, afatinib and T-DM1. (E) Tumor volume changes among mice treated with vehicle, and pyrotinib, afatinib and T-DM1 by 24 days. (F) Body weight changes among mice treated with vehicle, pyrotinib, afatinib and T-DM1. (G) Concentrations in plasma and in tumor in different doses of pyrotinib treatment groups were detected on day 24 after administration. The pyrotinib concentration in the tumor of the 80 mg/kg group was not available due to a low volume of tumor tissue after 24 days of pyrotinib treatment. (H) Concentrations in plasma and in tumor of pyrotinib and afatinib treatment groups were detected on day 24 after administration. (I) IHC staining of HER2 and its downstream proteins including ERK and Akt, in vehicle and pyrotinib treatment groups. \* $P < 0.05$ ; \*\* $P < 0.01$ ; \*\*\* $P < 0.001$ ; \*\*\*\* $P < 0.0001$ .

insufficiency. CT scan showed sustained tumor shrinkage after 1, 6 and 12 months of therapy (Figure 4E). The second patient was a 53-year-old Chinese male who was diagnosed with T4N2M1a stage IV lung adenocarcinoma with pleural and pericardial metastases. Direct sequencing revealed A775\_G776insYVMA in exon 20 of HER2. He initially received carboplatin and pemetrexed chemotherapy followed by afatinib (40 mg once daily), but eventually progressed on both lines of treatment. Therefore, he enrolled in this pyrotinib trial and had a partial response to pyrotinib 400 mg oral daily (Figure 4F).

## Discussion

HER2 exon 20 mutations represent 2%–3% of NSCLC patients, and currently chemotherapy remains to be the main therapeutic strategy [9, 13]. Here, we generated an HER2<sup>YVMA</sup> insertion patient-derived organoid model and a PDX model. We found that when compared with afatinib, T-DM1 or lower dose

pyrotinib, higher dose pyrotinib inhibited the growth of HER2-mutant cancer in both the HER2<sup>YVMA</sup> insertion patient-derived organoid and PDX models. Finally, we provided clinical evidence of the activity of pyrotinib (400 mg, p.o. once daily) in 15 patients with HER2-mutant NSCLC with an ORR of 53.3% and a median PFS of 6.4 months in our phase II study.

Insertions in exon 20 of *HER2* consists of multiple variants, ranging from 3 to 12 bp long [4, 5], and a previous study found that the clinical and biochemical heterogeneity among *HER2* mutations affected sensitivity to anti-HER2 TKIs [19]. Thus, using patient-derived tumors to generate cell lines and animal models is essential to test the potential of novel compounds for future therapeutic interventions [20]. Our study generated a patient-derived organoids model that harbored the most frequent HER2-mutant variant, A775\_G776insYVMA, and found that the drug response observed in the organoids was highly consistent with that of HER2<sup>YVMA</sup> PDX model. In line with our results, several groups have demonstrated the applicability of organoid models to study patient populations with rare mutations [17, 20, 21]. Vlachogiannis et al. [22] compared responses



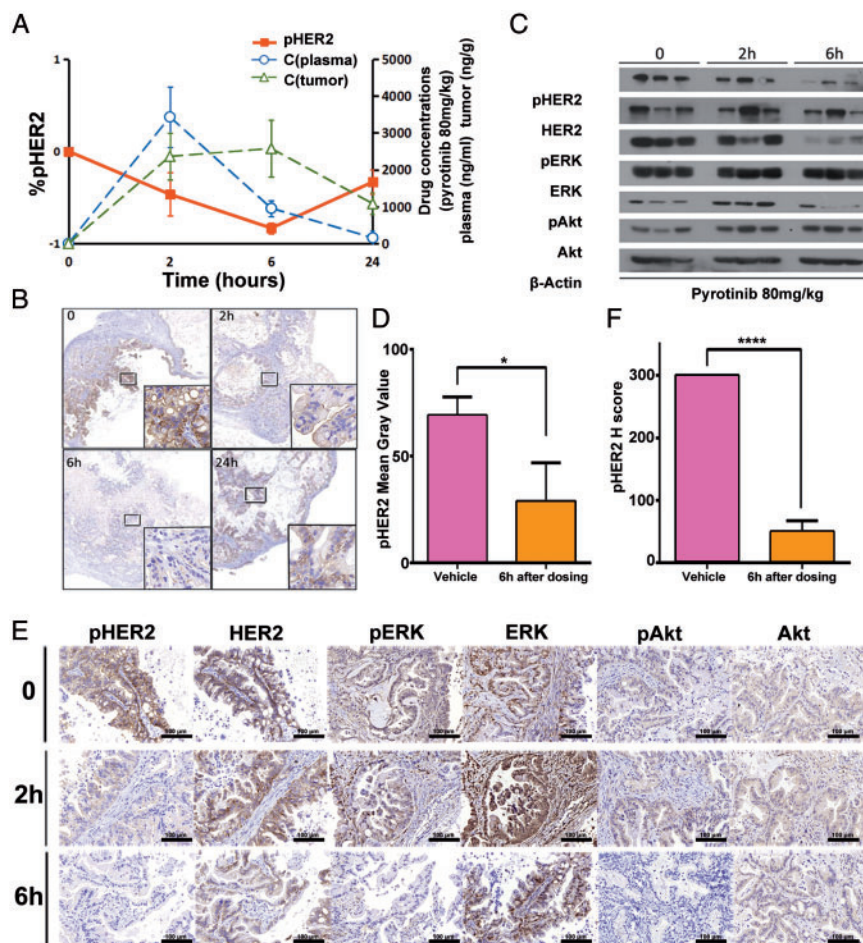


**Figure 3.** PK/PD correlation of pyrotinib in PDX model. (A) Concentrations of pyrotinib in plasma and in tumor were detected at 0, 2, 6, 24 h after dosing. Pyrotinib plasma concentrations peaked at ~2 h after dosing. Concentration of pyrotinib in tumor reached a relative maximum at 6 h, and at the same time, pHER2 was maximally inhibited. (B) Representative images of pHER2 in tumor tissues at 0, 2, 6, 24 h after pyrotinib treatment. (C, D) Western blot analyzed the proteins of HER2 and its downstream proteins including ERK and Akt in mice treated with pyrotinib (80 mg/kg) at 0, 2, 6 h after dosing. Phosphorylation of these proteins was significantly inhibited 6 h after dosing. (E, F) IHC analyzed the proteins of HER2 and its downstream proteins including ERK and Akt in mice treated with pyrotinib (80 mg/kg) at 0, 2, 6 h after dosing. Phosphorylation of these proteins was significantly inhibited 6 h after dosing. \* $P < 0.05$ ; \*\* $P < 0.01$ ; \*\*\* $P < 0.001$ ; \*\*\*\* $P < 0.0001$ .

with anticancer agents in organoids with the response of the patients in clinical trials, and their results suggested that patient-derived organoids can recapitulate patient responses.

Our observations indicate that all three anti-HER2 drugs, afatinib, T-DM1 and pyrotinib can block HER2 downstream signaling pathways. Among them, pyrotinib was the most potent at inhibiting tumor growth *in vitro* and *in vivo* using clinically relevant concentration. Furthermore, in our HER2 PDX model, high dose of pyrotinib (80 mg/kg, once daily) resulted in 52.2% tumor burden reduction in 24 days, whereas lower doses of pyrotinib did not lead to consistent tumor shrinkage, suggesting that the anticancer effect of pyrotinib is dose dependent. This is reminiscent of an earlier study using afatinib, which showed that pulse afatinib resulted in better responses in patients with HER2 exon 20 insertion mutated lung adenocarcinoma [23]. We also observed a strong inhibition of pHER2 after 6 h of treatment with high dose pyrotinib. Taken together, these data indicate that high dose pyrotinib demonstrated a robust anticancer effect both

*in vitro* and *in vivo*. Although pyrotinib dose of 80 mg/kg in the PDX model looks high, it is in fact corresponding to the recommended phase II dose (RP2D) in human [16] [(RP2D<sub>pyrotinib</sub>: 400 mg/kg)/60 kg  $\times$  12.3 = 82mg/kg, 60 kg was taken as the average body weight and 12.3 was the correction factor (Km)] based on the FDA guidelines for the conversion of drug dose between human and animals[24], which is reflected by its faster metabolism in mice ( $t_{1/2}$  = 5.37; [supplementary Table S3](#), available at *Annals of Oncology* online).

Dose-limiting toxicity of afatinib results in insufficient clinically available doses of afatinib and low plasma concentrations that barely achieve preclinical model inhibition. A retrospective cohort study failed to repeat the response rate [11] despite encouraging results of several reports [8, 25]. Further investigation found that, in an HER2 exon 20 insertion mutated lung cancer cell line, afatinib exhibited a 50% higher inhibitory concentration than was achieved by afatinib 40 mg daily, the licensed dose for patients with NSCLC [23]. A phase I clinical study of pyrotinib

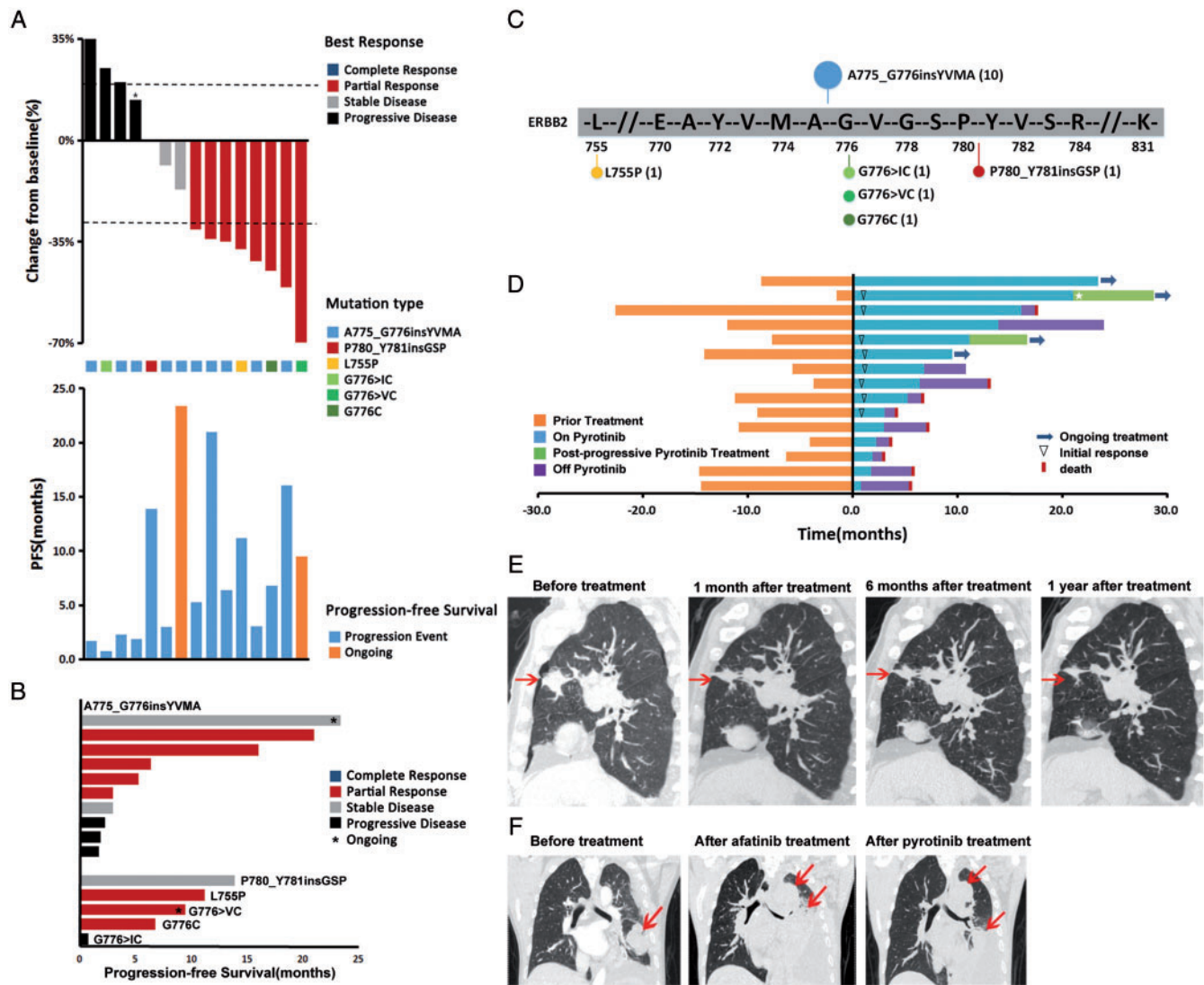


**Figure 4.** HER2-mutant lung cancer patients response to pyrotinib. (A, B) Percent best change from baseline of target lesions and progression-free survival (PFS) plots corresponding to each type of HER2 mutations. \*The target lesions of this patient increased by <20% while the nontarget lesions progressed, so we evaluated this as progressive disease. (C) Distribution of HER2 mutations observed in the cohort of 15 patients. (D) Treatment time of 15 patients in this study. Prior treatment: Time from diagnosis of advanced NSCLC or relapse. ☆, this patient had received one cycle of albumin bound-paclitaxel (100 mg i.v.gtt, D1) during postprogressive pyrotinib treatment. (E) Computed tomography (CT) scan of a 78-year-old patient with HER2-A775\_G776YVMA-inserted advanced lung cancer. His lung lesions were significantly reduced after pyrotinib treatment and CT scan showed sustained tumor shrinkage. (F) CT scan of a 53-year-old patient with HER2-A775\_G776YVMA-inserted advanced lung cancer. He responded to pyrotinib after disease progression on afatinib.

demonstrated that a 400 mg daily dose was tolerable and achieved a plasma concentration of 147 ng/ml and a  $AUC_{0-24h}$  of 1860 ng h/ml [16], significantly higher than the plasma concentrations reported for afatinib (21.1 ng/ml, 662 ng h/ml) [18], dacomitinib (25.9 ng/ml, 421 ng h/ml) [26] and neratinib (75.9 ng/ml, 823 ng h/ml) [27] in other phase I clinical trials (supplementary Table S7, available at *Annals of Oncology* online). Pyrotinib also has a higher log *P* (oil–water partition coefficient) of 4.475 than afatinib (3.101), dacomitinib (3.970) and neratinib (3.866), suggesting that pyrotinib is more lipophilic, which could result in better passive absorption and less gastrointestinal adverse effects such as diarrhea (supplementary Table S8, available at *Annals of Oncology* online). Consistent with these findings, we

found that the average plasma drug concentration of mice treated with 80 mg/kg-pyrotinib (2316.7 ng/ml) was significantly higher than that of mice in afatinib group (76.9 ng/ml). Despite this high blood concentration, the administered mice experienced no significant decrease in body weight. And high dose pyrotinib showed better tolerability when compared with afatinib. Again, this 80 mg/kg dose in mice matches the 400 mg daily dose in human based on human–animal dose conversion per FDA guideline [24], and is therefore clinically relevant.

These findings suggest that patients with *HER2* exon 20 mutations may receive great clinical benefit from pyrotinib treatment. This hypothesis is supported by a respectable efficacy signal (ORR 53.3% and median PFS of 6.4 months) and good

tolerability (no grade 3 or 4 adverse events) in the 15 patients enrolled in the phase II trial of pyrotinib 400 mg a day. These results demonstrate that pyrotinib has potent antitumor activity against *HER2* exon 20 mutant NSCLC, and support further clinical testing of pyrotinib in NSCLC patients with *HER2* exon 20 mutations to determine its impact on the overall survival, response rate, duration of response, as well as safety and toxicity. We initiated a multi-center phase II trial (NCT02834936) afterwards, currently in progress. Recently, it was released that poziotinib and TAK-788 (AP32788) also showed promising results in preclinical model together with early clinical setting [28, 29], despite only one PR in *HER2* mutation cohort in TAK-788 dose-escalation phase [30]. Jang et al. [31] also reported a new *HER2* Ex20Ins mutant inhibitor that was highly potent *in vitro*. Patients with *HER2* exon 20 mutations might enter into the era of targeted therapy in the near future.

In conclusion, compared with licensed drugs with anti-*HER2* activity (i.e. afatinib and T-DM1), pyrotinib showed greater potential to inhibit growth of lung cancers with *HER2* exon 20 mutations in an organoid model and a PDX model. In patients, pyrotinib is well-tolerated and showed promising effect in a phase II clinical study at a dose of 400 mg once daily. Pyrotinib's encouraging antitumor activity in patients with *HER2* exon 20 mutant lung cancers warrants further evaluation in an ongoing multi-center phase II trial.

## Funding

This study was supported in part by grants from the National Natural Science Foundation of China (No. 81772467), from the 'Shuguang Program' supported by Shanghai Education Development Foundation and Shanghai Municipal Education Commission (No. 16SG18), from the projects of the Science and Technology Commission of Shanghai Municipality (No. 16411964600), from the Development Fund for Shanghai Talents (No. 201558) and the University of Iowa Start-up Funds (JZ), as well as the Grant IRG-15-176-40 from the American Cancer Society, administered through The Holden Comprehensive Cancer Center at The University of Iowa (JZ). The funding body had no role in the design of the study and collection, analysis and interpretation of data and in writing the manuscript.

## Disclosure

The authors have declared no conflicts of interest.

## References

- Shigematsu H, Takahashi T, Nomura M et al. Somatic mutations of the *HER2* kinase domain in lung adenocarcinomas. *Cancer Res* 2005; 65(5): 1642–1646.
- Buttitta F, Barassi F, Fresu G et al. Mutational analysis of the *HER2* gene in lung tumors from Caucasian patients: mutations are mainly present in adenocarcinomas with bronchioloalveolar features. *Int J Cancer* 2006; 119(11): 2586–2591.
- Tomizawa K, Suda K, Onozato R et al. Prognostic and predictive implications of *HER2/ERBB2/neu* gene mutations in lung cancers. *Lung Cancer* 2011; 74(1): 139–144.
- Arcila ME, Chaft JE, Nafa K et al. Prevalence, clinicopathologic associations, and molecular spectrum of *ERBB2* (*HER2*) tyrosine kinase mutations in lung adenocarcinomas. *Clin Cancer Res* 2012; 18(18): 4910–4918.
- Kris MG, Johnson BE, Berry LD et al. Using multiplexed assays of oncogenic drivers in lung cancers to select targeted drugs. *JAMA* 2014; 311(19): 1998–2006.
- Mazieres J, Peters S, Lepage B et al. Lung cancer that harbors an *HER2* mutation: epidemiologic characteristics and therapeutic perspectives. *J Clin Oncol* 2013; 31: 1997–2003.
- Li X, Zhao C, Su C et al. Epidemiological study of *HER-2* mutations among *EGFR* wild-type lung adenocarcinoma patients in China. *BMC Cancer* 2016; 16(1): 828.
- De Grève J, Teugels E, Geers C et al. Clinical activity of afatinib (BIBW 2992) in patients with lung adenocarcinoma with mutations in the kinase domain of *HER2/neu*. *Lung Cancer* 2012; 76(1): 123–127.
- Kris MG, Camidge DR, Giaccone G et al. Targeting *HER2* aberrations as actionable drivers in lung cancers: phase II trial of the pan-*HER* tyrosine kinase inhibitor dacomitinib in patients with *HER2*-mutant or amplified tumors. *Ann Oncol* 2015; 26(7): 1421–1427.
- Gandhi L, Bahleda R, Tolaney SM et al. Phase I study of neratinib in combination with temsirolimus in patients with human epidermal growth factor receptor 2-dependent and other solid tumors. *J Clin Oncol* 2014; 32(2): 68–75.
- Mazieres J, Barlesi F, Filleron T et al. Lung cancer patients with *HER2* mutations treated with chemotherapy and *HER2*-targeted drugs: results from the European EUHER2 cohort. *Ann Oncol* 2016; 27(2): 281–286.
- Hyman DM, Piha-Paul SA, Won H et al. *HER* kinase inhibition in patients with *HER2*- and *HER3*-mutant cancers. *Nature* 2018; 554(7691): 189–194.
- Eng J, Hsu M, Chaft JE et al. Outcomes of chemotherapies and *HER2* directed therapies in advanced *HER2*-mutant lung cancers. *Lung Cancer* 2016; 99: 53–56.
- Wang Y, Zhang S, Wu F et al. Outcomes of pemetrexed-based chemotherapies in *HER2*-mutant lung cancers. *BMC Cancer* 2018; 18(1): 326.
- Li X, Yang C, Wan H et al. Discovery and development of pyrotinib: a novel irreversible *EGFR/HER2* dual tyrosine kinase inhibitor with favorable safety profiles for the treatment of breast cancer. *Eur J Pharm Sci* 2017; 110: 51–61.
- Ma F, Li Q, Chen S et al. Phase I study and biomarker analysis of pyrotinib, a novel irreversible pan-ErbB receptor tyrosine kinase inhibitor, in patients with human epidermal growth factor receptor 2-positive metastatic breast cancer. *J Clin Oncol* 2017; 35(27): 3105–3112.
- Gao D, Vela I, Sboner A et al. Organoid cultures derived from patients with advanced prostate cancer. *Cell* 2014; 159(1): 176–187.
- Yap TA, Vidal L, Adam J et al. Phase I trial of the irreversible *EGFR* and *HER2* kinase inhibitor BIBW 2992 in patients with advanced solid tumors. *J Clin Oncol* 2010; 28(25): 3965–3972.
- Kosaka T, Tanizaki J, Paranal RM et al. Response heterogeneity of *EGFR* and *HER2* Exon20 insertions to covalent *EGFR* and *HER2* inhibitors. *Cancer Res* 2017; 77(10): 2712–2721.
- Pauli C, Hopkins BD, Prandi D et al. Personalized in vitro and in vivo cancer models to guide precision medicine. *Cancer Discov* 2017; 7(5): 462–477.
- Verissimo CS, Overmeer RM, Ponsioen B et al. Targeting mutant *RAS* in patient-derived colorectal cancer organoids by combinatorial drug screening. *Elife* 2016; 5: e18489.
- Vlachogiannis G, Hedayat S, Vatsiou A et al. Patient-derived organoids model treatment response of metastatic gastrointestinal cancers. *Science* 2018; 359(6378): 920–926.
- Costa DB, Jorge SE, Moran JP et al. Pulse afatinib for *ERBB2* exon 20 insertion mutated lung adenocarcinomas. *J Thorac Oncol* 2016; 11(6): 918–923.
- The Office of New Drugs in the Center for Drug Evaluation and Research (CDER) at the Food and Drug Administration. Guidance for Industry:



- Estimating the Maximum Safe Starting Dose in Adult Healthy Volunteer. U.S. Food and Drug Administration 2005.
25. Peters S, Curioni-Fontecedro A, Nechushtan H et al. Activity of afatinib in heavily pretreated patients with ERBB2 mutation-positive advanced NSCLC: findings from a global named patient use program. *J Thorac Oncol* 2018; 11: 1897–1905.
  26. Jänne PA, Boss DS, Camidge DR et al. Phase I dose-escalation study of the pan-HER inhibitor, PF299804, in patients with advanced malignant solid tumors. *Clin Cancer Res* 2011; 17(5): 1131–1139.
  27. Wong KK, Fracasso PM, Bukowski RM et al. A phase I study with neratinib (HKI-272), an irreversible pan ErbB receptor tyrosine kinase inhibitor, in patients with solid tumors. *Clin Cancer Res* 2009; 15(7): 2552–2558.
  28. Robichaux JP, Elamin YY, Tan Z et al. Mechanisms and clinical activity of an EGFR and HER2 exon 20-selective kinase inhibitor in non-small cell lung cancer. *Nat Med* 2018; 24(5): 638–646.
  29. Gonzalez F, Zhu X, Huang WS et al. AP32788, a potent, selective inhibitor of EGFR and HER2 oncogenic mutants, including exon 20 insertions, in preclinical models. *Cancer Res* 2016; 76(Suppl 14): 2644.
  30. Doebele RC, Riely GJ, Spira AI et al. First report of safety, PK, and preliminary antitumor activity of the oral EGFR/HER2 exon 20 inhibitor TAK-788 (AP32788) in non-small cell lung cancer (NSCLC). *J Clin Oncol* 2018; 36(Suppl 15): 9015–9015.
  31. Jang J, Son J, Park E et al. Discovery of a highly potent and broadly effective epidermal growth factor receptor and HER2 exon 20 insertion mutant inhibitor. *Angew Chem Int Ed Engl* 2018; 57(36): 11629–11633.